

# Directed Partial Correlation: Inferring Large-Scale Gene Regulatory Network through Induced Topology Disruptions

Yinyin Yuan<sup>1,2\*</sup>, Chang-Tsun Li<sup>3</sup>, Oliver Windram<sup>4</sup>

**1** Cancer Research UK, Cambridge Research Institute, Cambridge, United Kingdom, **2** Department of Oncology, University of Cambridge, Cambridge, United Kingdom, **3** Department of Computer Science, University of Warwick, Coventry, United Kingdom, **4** Warwick Horticulture Research Institute, University of Warwick, Wellesbourne, United Kingdom

## Abstract

Inferring regulatory relationships among many genes based on their temporal variation in transcript abundance has been a popular research topic. Due to the nature of microarray experiments, classical tools for time series analysis lose power since the number of variables far exceeds the number of the samples. In this paper, we describe some of the existing multivariate inference techniques that are applicable to hundreds of variables and show the potential challenges for small-sample, large-scale data. We propose a directed partial correlation (DPC) method as an efficient and effective solution to regulatory network inference using these data. Specifically for genomic data, the proposed method is designed to deal with large-scale datasets. It combines the efficiency of partial correlation for setting up network topology by testing conditional independence, and the concept of Granger causality to assess topology change with induced interruptions. The idea is that when a transcription factor is induced artificially within a gene network, the disruption of the network by the induction signifies a gene's role in transcriptional regulation. The benchmarking results using GeneNetWeaver, the simulator for the DREAM challenges, provide strong evidence of the outstanding performance of the proposed DPC method. When applied to real biological data, the inferred starch metabolism network in *Arabidopsis* reveals many biologically meaningful network modules worthy of further investigation. These results collectively suggest DPC is a versatile tool for genomics research. The R package DPC is available for download (<http://code.google.com/p/dpcnet/>).

**Citation:** Yuan Y, Li C-T, Windram O (2011) Directed Partial Correlation: Inferring Large-Scale Gene Regulatory Network through Induced Topology Disruptions. PLoS ONE 6(4): e16835. doi:10.1371/journal.pone.0016835

**Editor:** Diego Di Bernardo, Fondazione Telethon, Italy

**Received:** August 24, 2010; **Accepted:** January 11, 2011; **Published:** April 6, 2011

**Copyright:** © 2011 Yuan et al. This is an open-access article distributed under the terms of the Creative Commons Attribution License, which permits unrestricted use, distribution, and reproduction in any medium, provided the original author and source are credited.

**Funding:** This work was supported by the Department of Computer Science at the University of Warwick through a PhD Studentship for Yinyin Yuan to conduct the work under Chang-Tsun Li's supervision. Oliver Windram is supported by Warwick HRI. The funders had no role in study design, data collection and analysis, decision to publish, or preparation of the manuscript.

**Competing Interests:** The authors have declared that no competing interests exist.

\* E-mail: yy341@cam.ac.uk

## Introduction

In recent years various multivariate analysis techniques have been developed for inferring causal relations among time series. Although many of them have previously proved their power on analysing economic and neurophysiological data, the unique nature of gene expression time series, typically large-scale and small-sample, poses a challenge to these techniques. On the other hand, gene expression dynamics are important, since they directly reveal the active components within the cell over time, indicating gene regulatory relationships at the transcriptional level. Therefore, a lot of time and effort has been spent on developing tools that suit the need for expression time series analysis.

We define a causal relation as a target at the current time having directed dependence on a regulator at the past time, when conditioned on the rest of the regulators (Figure 1(a)). Inferring causal relations between variables, when applied on gene expression data, is equivalent to inferring transcriptional regulatory relationships. Collectively, the complete set of regulatory relationships among genes leads to the reconstruction of gene regulatory networks. The resulting networks or network modules (Figure 1(b)), if evaluated together with biological knowledge,

should provide new insights into the dynamics and functioning of the regulatory system (Figure 1(c)).

For example, a directed network inference approach, termed the shrinkage vector autoregressive method (SVAR), was proposed by Rhein *et al.* [1]. The class of shrinkage methods, which effectively shrink the effects from some predictors to zero, can both improve performance and reduce computational costs in many instances. In particular, SVAR is designed specifically for gene expression data to circumvent the small sample problem. Also, dynamic Bayesian networks (DBNs) [2,3], a class of commonly used graphical models, have also been applied in this research area. Another recent advance in this area was the introduction of the concept of Granger causality [4] which is well known in economics for causal inference on time series data [5,6]. For example, Zou *et al.* [5] compare DBNs and a method based on Granger causality and conclude that while the method based on Granger causality performs better with sufficiently large datasets (thousands of samples), DBNs are more likely to perform well on small-sample datasets (as is often the case in microarray experiments).

In this paper, we describe some of the most commonly used multivariate inference techniques for large-scale gene regulatory

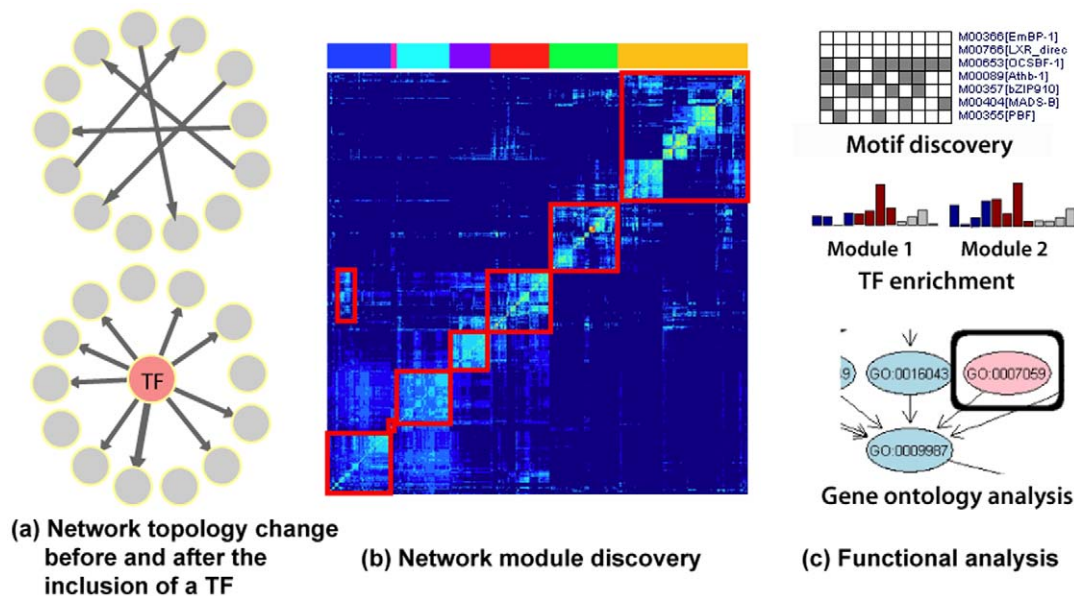


**Figure 1. DPC for large-scale transcriptional regulatory network inference.** (a) DPC detects network topology changes with the addition of a gene, the inclusion of a transcription factor should lead to dramatic changes of the connectivity of its downstream targets, (b) module discovery in the large-scale DPC network by biclustering the network adjacency matrix, (c) functional analysis of the network modules reveals putative transcription factors active under the biological condition.  
doi:10.1371/journal.pone.0016835.g001

network reconstruction. We demonstrate that the proposed directed partial correlation (DPC) algorithm is an efficient and effective solution to causal/regulatory network inferences on small-sample, large-scale gene expression data. The comprehensive analysis of the experimental results not only reveals good accuracy of the proposed DPC method in large-scale prediction, but also gives much insight into all methods under evaluation.

In essence, partial correlation, which is able to test conditional independence on multivariate Gaussian data, is used as the mathematical foundation for establishing direct interactions among genes. For example, variable *b* is highly correlated with *c* because of the causal effects from *a* (Figure 2(a)). Pearson correlation may give rise to many false positives as in Figure 2(c), and Figure 2(b) may be probable for methods that do not account for conditional independence. However, partial correlation tests the correlation between two variables after the linear effects from the rest of the data are removed, hence no relationship exists between *b* and *c* after the effect from *a* is removed. (Note that partial correlation only infers undirected relationships, unlike what are shown in Figure 2.) Conditional independence, although by itself is insufficient to denote a causal link, can be a powerful tool for removing indirect relationships. Therefore, when inferring the relationship between two gene expression profiles, the other

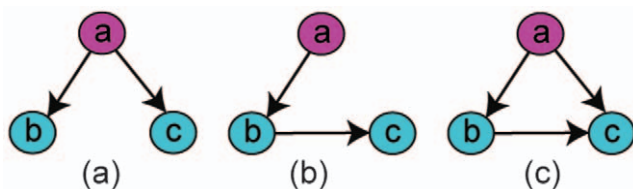


**Figure 2. Possible inference results of the causal relations among three variables.** (a) True/direct interactions, (b) indirect interaction inference, (c) bivariate inference.  
doi:10.1371/journal.pone.0016835.g002

expression profiles can be taken into account to discriminate between direct (Figure 2(a)) and indirect (Figure 2(b) and (c)) interactions.

Although a shrinkage estimate of partial correlation [7] is computationally fast and well suited for small sample data analysis [8], the inferred interactions are undirected. In an undirected network, the role that a gene plays in different regulatory activities is unknown. Therefore, based on partial correlation, we propose a directed approach specifically targeted at small-sample gene expression data. It is then compared with some of the existing methods, DBNs, SVAR, and GC-VAR, to demonstrate its effectiveness.

An immediate difficulty in accessing a network inference method lies in the fact that current biological knowledge is far from sufficient to provide a clear picture. A reasonable validation process involves the use of real biological datasets, in addition to synthetic datasets which provide both ground truth and unlimited sample length. Under a broad set of assumptions, if datasets of various sample sizes and number of variables can be produced, an inference method then can be tested extensively, especially against its sensitivity to dimensionality. We adopt this validation process, but specifically note that, since most of the methods are probabilistic, selecting cutoffs to represent one resulting network may introduce false positives. Hence it is desirable to compare different methods with their direct output – the network probability matrix in which a coefficient denotes the probability of interaction between two genes.

The rest of this paper is organised as follows. In the second section, we present the technical details of the three existing algorithms, together with the proposed algorithm for directed regulatory network inference. Then benchmarking using datasets of various sizes generated by GeneNetWeaver [9] is presented. GeneNetWeaver provides simulations for DREAM (The Dialogue for Reverse Engineering Assessments and Methods) [10] *in silico* challenges. DREAM is a community effort to assess reverse engineering algorithms. Benchmarking using GeneNetWeaver

datasets should provide strong evidence of the power of network inference algorithm in a controlled environment. Specifically, we discuss the statistical properties of transcriptional networks and their impacts on the performance of an algorithm in the comparative evaluation. In addition, we discuss model assumptions for different inference methods. The question is, to what extent the model assumptions influence the confidence of the inference outcome.

The experiments are designed to give a thorough evaluation of the proposed algorithm and to compare the four algorithms in a coherent manner. The reported results on simulated data indicate superior performance of the proposed algorithm both in terms of accuracy and efficiency. For the biological dataset, detailed analysis of the results suggests that DPC uncovers more biologically relevant regulatory relationships than the competing method SVAR.

## Methods

In this section, we hope to shed some light on the nature of different inference techniques, their advantages and inherent problems. First the autoregressive models are presented, they form the theoretical ground for most of the existing methods in comparison. Then we describe the technical details for the three representative existing methods, with notes on their capabilities in gene expression analysis. Next, the proposed DPC method is formulated. These technical details provide us with a strong foundation for later discussions of experimental results.

### Existing multivariate time series inference methods

**Vector autoregressive models (VAR).** Suppose  $\mathbf{Y} = \{\mathbf{y}_i | i=1,2,\dots,n\}$  is a multivariate stationary time series consisting of  $n$  variables and  $\tau$  time points. A  $p$ -order vector autoregressive VAR( $p$ ) model specifies that the value of the  $i$ th variable at a time point  $t$ ,  $y_i(t)$ , is a linear combination of a constant/mean value, the past of the multivariate time series, and a noise component

$$\mathbf{Y}(t) = \mathbf{B} + \mathbf{A} \sum_{u=1}^p \mathbf{Y}(t-u) + \xi(t). \quad (1)$$

$\mathbf{B}$  is a constant matrix of length  $n$ .  $\xi$  consists of vectors of residuals  $\{\xi_i | i=1..n\}$ , each assumed to be zero mean noise with variance  $\sigma_i^2$ .  $\mathbf{A}$  is the  $n \times n$  coefficient matrix representing the dynamic structure. When  $\mathbf{A}$  is a constant matrix, this model assumes homogeneity across time. A special case of the  $p$ -order VAR process, the first-order autoregressive model (VAR(1)), is often considered when analysing short microarray time series [1,3]

$$\mathbf{Y}(t) = \mathbf{B} + \mathbf{A}\mathbf{Y}(t-1) + \xi(t). \quad (2)$$

**Granger causality inference method based on VAR model (GC-VAR).** Time series  $a$  is said to Granger cause time series  $b$  if the forecast of  $b$  has incremental predictive power with the knowledge of the past state of  $a$  [4]. For the VAR models, a widely accepted measure of the predictive power of  $a$  on  $b$  is the variance of the residuals as a result of model fitting [4,11]. Informally, the method measures the influence of one time series on another by checking if the prediction of the response can be improved by incorporating the knowledge of the past of a predictor. One of the first attempts for gene expression data analysis is a bivariate model

that uses Granger causality to infer relationships between pairs of variables without taking into account other variables [12]. For comparative purposes, we implemented a multivariate model, since the bivariate model could lead to false positive edges such as the ones in Figure 2(c), compared with the true network (Figure 2(a)).

In the multivariate case. Let  $\mathbf{Y}^-$  symbolise the past state of  $\mathbf{Y}$ ,  $\mathbf{Y}^- = \{\mathbf{Y}(u) | u=1,\dots,\tau-1\}$ , and let  $\mathbf{y}_i^-$  symbolise the past of variable  $\mathbf{y}_i$ . Based on Granger causality, the prediction power of one variable  $\mathbf{y}_i$  on the other variable  $\mathbf{y}_j$ ,  $i \neq j$ , can be measured by

$$g_{y_i \rightarrow y_j} = \ln \left( \frac{\sigma_{y_j | \mathbf{Y}^-}^2}{\sigma_{y_j | \mathbf{Y}_i^-}^2} \right). \quad (3)$$

Symbol “|” denotes operation “condition on” and symbol “/” denotes “without”.  $\sigma_{y_j | \mathbf{Y}^-}$  is the variance of the residual  $\xi(t)$  in the VAR(1) model for  $\mathbf{y}_j$  conditioned on the past of all variables  $\mathbf{Y}^-$ . It is compared to  $\sigma_{y_j | \mathbf{Y}_i^-}$  which is conditioned on the past of all variables but  $\mathbf{y}_i$ ,  $\mathbf{Y}_i^-$ . This method based on Granger Causality and the VAR model directly measures the prediction power of  $\mathbf{y}_i$  for  $\mathbf{y}_j$ , as a result of the reduction of prediction errors by incorporating  $\mathbf{y}_i$  into the VAR(1) model for  $\mathbf{y}_j$ . In other words, if introducing  $\mathbf{y}_i$  significantly reduces the variance of the prediction error of  $\mathbf{y}_j$ , then a variable  $\mathbf{y}_i$  Granger causes the variable  $\mathbf{y}_j$ . Since it requires fitting the autoregressive model with all variables and their past states, GC-VAR can only be applied to data satisfying:  $\tau > n(p+1)$ , indicating its limited potential in gene expression analysis.

**Shrinkage VAR method (SVAR).** Although the VAR model has been widely used in economics and neuroscience, it has its own limitations when small samples are encountered. An effective shrinkage estimation procedure was developed for learning the VAR models from small sample data [1]. The idea is that a shrinkage estimate can replace the covariance matrix for the joint matrix of both the present state and the past state(s), which then leads to the computation for regression coefficients. The basic procedure consists of first computing the shrinkage estimates of covariance matrices to obtain regression coefficients. Then instead of using the regression coefficients directly, the corresponding partial correlation coefficients are statistically tested. Significant coefficients are then selected using False Discovery Rate (FDR) [13] to be included in the reconstructed network.

The covariance matrix would otherwise be ill-conditioned, given the large number of variables ( $2 \times n$ ) and short time series  $\tau, \tau \ll n$ . Let  $\Phi$  denote the joint matrix of the multivariate  $\mathbf{Y}$ 's present state ( $\mathbf{Y}^+ = \{\mathbf{Y}(u) | u=2,\dots,\tau\}$ ) and past state with a time lag of 1 time point ( $\mathbf{Y}^- = \{\mathbf{Y}(u) | u=1,\dots,\tau-1\}$ ),  $\Phi = [\mathbf{Y}^+ \mathbf{Y}^-]$ . Assuming that the data has zero mean, an unbiased estimate of the covariance matrix for  $\Phi$  is

$$\begin{aligned} \text{cov}(\Phi) &= \frac{1}{\tau-1} [\mathbf{Y}^+ \mathbf{Y}^-]' [\mathbf{Y}^+ \mathbf{Y}^-] \\ &= \frac{1}{\tau-1} \begin{bmatrix} \mathbf{Y}^{++} & \mathbf{Y}^{+-} \\ \mathbf{Y}^{-+} & \mathbf{Y}^{--} \end{bmatrix}. \end{aligned} \quad (4)$$

Note that this matrix contains the sub-matrices  $\mathbf{Y}^- \mathbf{Y}^-$  and  $\mathbf{Y}^- \mathbf{Y}^+$ . Meanwhile, the ordinary least squares (OLS) estimation [14] for the regression coefficient  $\mathbf{A}$  in the VAR(1) model (Eq. (2)) is:

$$\hat{\mathbf{A}}^{(1)} = (\mathbf{Y}'\mathbf{Y})^{-1}\mathbf{Y}'\mathbf{Y}^+ \tag{5}$$

Therefore, the shrinkage estimation of  $cov(\Phi)$  will lead to the estimated coefficient matrix  $\hat{\mathbf{A}}$ . Then the partial correlation coefficients  $q$  can be computed from  $\hat{\mathbf{A}}$  and the FDR is used to select significant coefficients. With large numbers of variables, this method gave good results in the comparative simulation study using simulated autoregressive data in the original paper [1].

**Dynamic Bayesian Networks (DBNs).** DBNs are graphical models trained to maximise the joint probability of a set of observed data and their conditional dependencies. DBNs have been routinely applied to data, mainly long time series, to provide information about system dynamics. However, a major concern about DBNs is their inefficiency in large-scale prediction, i.e., with the presence of many variables.

DBNs implementations are usually designed for data with hundreds or thousands of samples. High costs of microarray experiments prohibit most of the techniques from exploring small sample gene expression data. In this paper, we use the implementation of the R package G1DBN [3], which is based on a trivariate AR(1) model:

$$\begin{aligned} \mathbf{Y}(1) &\sim \mathcal{N}(\mu_1, \sum_1), \\ \mathbf{Y}(t) &= \mathbf{B} + \mathbf{A}\mathbf{Y}(t-1) + \varepsilon(t), \\ \varepsilon(t) &\sim \mathcal{N}(0, \sigma^2), \end{aligned} \tag{6}$$

with predefined  $\mu_1, \sum_1$ , and  $\sigma^2$ . This method measures the conditional dependence between two variables  $\mathbf{y}_i, \mathbf{y}_j$  by testing the null hypothesis  $H_0^{i,j,k} : "a_{ijk} = 0"$  on every third variable  $\{\mathbf{y}_k | k \neq i, j\}$ . Then, a score is assigned to the potential edge  $\mathbf{y}_i \rightarrow \mathbf{y}_j$  corresponding to the maximum  $p$ -values from the tests  $p_{\max}(\mathbf{y}_i \rightarrow \mathbf{y}_j)$ . This means the algorithm has a computational complexity of  $\mathcal{O}(n^3)$ . The computation of this method may be too heavy for data with more than a hundred variables.

**Proposed directed partial correlation inference method (DPC)**

The shrinkage estimate for partial correlation in [7] was formulated specifically for the inference from small sample gene expression data. Although partial correlation is undoubtedly fast in computation and suitable for small sample problem, it can only infer undirected networks. Another problem is that variable time lag cannot be taken into account as in a VAR(1) model. We introduce the notion of directed partial correlation (DPC) for fast inference of directed gene networks. The idea is similar to the idea behind Granger causality – a variable  $a$  has causal influence on another variable  $b$ , if the removal/addition of  $c$  has a large impact on the prediction of  $b$ . While GC-VAR measures this impact by comparing the residuals before and after adding  $a$  to the prediction of  $b$ , DPC measures it by examining the correlation coefficients.

**Zero-order directed partial correlation DPC(0).** Directed partial correlation aims to investigate the effect of including a variable in the prediction of another gene, i.e. the change of dependencies among other genes. Let  $\mathbf{Q}_Y$  of size  $n \times n$  denote the partial correlation matrix for  $\mathbf{Y}$ . Each element  $q(i, j | \mathbf{Y})$  in  $\mathbf{Q}_Y$  is the partial correlation between  $\mathbf{y}_i$  and  $\mathbf{y}_j$  given  $\mathbf{Y}$ ,  $i, j = 1, \dots, n, i \neq j$ , i.e., the correlation between  $\mathbf{y}_i$  and  $\mathbf{y}_j$  after the linear effects of the rest of the variables are removed. This can be

formulated as  $q(i, j | \mathbf{Y})$ . The removal of linear effects from others means that the resulting partial correlation indicates the direct relationship between two variables. Figure 3(a) shows  $q(i, k | \mathbf{Y})$ ,  $k \neq i, j$ , which denotes the partial correlation between  $\mathbf{y}_i$  and  $\mathbf{y}_k$  when effects from all others, including  $\mathbf{y}_j$ , are removed.

However, the conditional dependence indicated by  $q(i, j | \mathbf{Y})$  is undirected. To investigate the influence  $\mathbf{y}_j$  has on  $\mathbf{y}_i$ , we propose the following. If we delete the variable  $\mathbf{y}_j$  from  $\mathbf{Y}$ , the partial correlation between  $\mathbf{y}_i$  and another variable  $\mathbf{y}_k, k \neq i, j$  is denoted as  $q(i, k | \mathbf{Y}_{-j})$  in the matrix  $\mathbf{Q}_{\mathbf{Y}_{-j}}$ . As shown in Figure 3(b), in the prediction of the relationship between  $\mathbf{y}_i$  and any other variable  $\mathbf{y}_k, k \neq i, j$ ,  $q(i, k | \mathbf{Y}_{-j})$  no longer remove the effect from  $\mathbf{y}_j$ , which means  $\mathbf{y}_j$  no longer take part in the prediction of  $\mathbf{y}_i$ . Consequently, there are two groups of statistics related to the prediction of  $\mathbf{y}_i$ , each corresponding to coefficients before and after the removal of  $\mathbf{y}_j$ . To be more specific, the first group is the  $i$  th row in  $\mathbf{Q}_Y$  without the  $i$  th and  $j$  th element,  $g_1 = \{q(i, j | \mathbf{Y}), j \neq i\}$ , shown in dark green in Figure 3(a). The second group corresponding to the dark green elements in Figure 3(b) is the  $i$  th row in  $\mathbf{Q}_{\mathbf{Y}_{-j}}$  without the  $i$  th element,  $g_2 = \{q(i, k | \mathbf{Y}_{-j}), j \neq i, k\}$ . Both groups have the length of  $n - 2$ . The effect  $\mathbf{y}_j$  has on the prediction of  $\mathbf{y}_i$  is defined as:

$$\begin{aligned} e_{\mathbf{y}_j \rightarrow \mathbf{y}_i}^{(0)} &= \mathbf{t}\text{-test}(g_1, g_2) \\ &= \mathbf{t}\text{-test}(\{q(i, k | \mathbf{Y}) | k \neq i, j\}, \{q(i, k | \mathbf{Y}_{-j}) | k \neq i, j\}). \end{aligned} \tag{7}$$

We use a paired t-test on the two groups to see if there is an effect on the prediction of other variables with the removal of variable  $\mathbf{y}_j$ . The null hypothesis is that there is no significant difference between the two groups, before and after the removal.

In summary, we take advantage of the fact that in computing partial correlation between two variables, all effects from other variables are removed. In other words,  $\mathbf{y}_j$  takes part in the predictions of  $\mathbf{y}_i$  with all other variables  $\mathbf{y}_k$ . We measure  $\mathbf{y}_j$ 's influence on  $\mathbf{y}_i$  by comparing partial correlation coefficients related to  $\mathbf{y}_i$  before and after the deletion of  $\mathbf{y}_j$ , since  $\mathbf{y}_j$  does not take part in the prediction of  $\mathbf{y}_i$  after the deletion.

**$p$ -order directed partial correlation DPC( $p$ ).** A key feature of the proposed DPC method is that it can be easily extended to include time lags. In the following discussion, we focus on first-order DPC ( $p = 1$ ) for the sake of simplicity, although the DPC algorithm can be generalized to any reasonable order  $p$ .

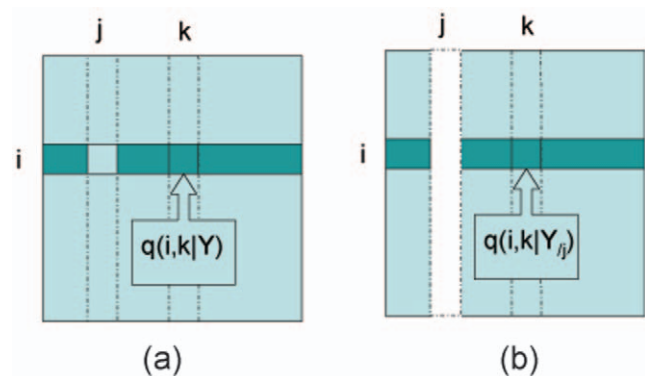


**Figure 3. Partial correlation matrices before and after deleting  $\mathbf{y}_j$ .** To predict  $\mathbf{y}_j$ 's influence on  $\mathbf{y}_i$ , two groups of partial correlation coefficients from two matrices (coloured dark green) are tested. (a) Coefficients in  $g_1$ , (b) Coefficients in  $g_2$ . doi:10.1371/journal.pone.0016835.g003



Note that  $p$  needs to be carefully chosen according to the microarray experimental design in order to capture the regulatory events.

Let  $\Phi$  be the joint matrix of the present state and the past state of data, i.e.,  $\Phi = [\mathbf{Y}^+ \mathbf{Y}^-]$ . To compute the correlation matrix for  $\Phi$ , we note that the covariance matrix of  $\Phi$  is ill-conditioned for small sample data and therefore not suitable. We use the shrinkage estimate method in Eq. (4) to compute the partial correlation matrix  $\mathbf{Q}_Y^{(1)}$  for  $\Phi$

$$\mathbf{Q}_Y^{(1)} = \begin{bmatrix} \mathbf{Q}^{++} & \mathbf{Q}^{+-} \\ \mathbf{Q}^{-+} & \mathbf{Q}^{--} \end{bmatrix}. \quad (8)$$

Hence each element in the sub-matrix  $\mathbf{Q}^{++}$ ,  $q^{(1)}(i, j)$  with  $i = 1 \dots n, j = 1 \dots n$ , stands for the partial correlation between  $\mathbf{y}_i$  and  $\mathbf{y}_j$ , when the effects of the present states of other variables and the past states of all variables are removed. If a variable  $\mathbf{y}_j$  is deleted from the joint matrix  $\Phi$ , the corresponding partial correlation matrix  $\mathbf{Q}_{Y_{/j}}^{(1)}$  has an equivalent meaning as described in the zero-order model, i.e. the effect of  $\mathbf{y}_j$  is not taken into account in the prediction of the other variables. The first-order directed partial correlation from  $\mathbf{y}_j$  to  $\mathbf{y}_i$  can be formulated as

$$e_{\mathbf{y}_k \rightarrow \mathbf{y}_i}^{(1)} = \mathbf{t}\text{-test}(\{q^{(1)}(i, j | \mathbf{Y}) | j \neq i\}, \{q^{(1)}(i, k | \mathbf{Y}_{/j}) | k \neq i, k\}). \quad (9)$$

Note that although the partial correlation matrix is of size  $2n \times 2n$ , only the sub-matrix  $\mathbf{Q}^{++}$  is used for computing  $e^{(1)}$ . The probability of the directed interaction is indicated by the resultant  $p$ -values. Using FDR, adjusted  $p$ -values are selected in accordance with confidence levels, for example, 2% of FDR means accepting all tests with adjusted  $p$ -values  $\leq 0.02$  as significant. The algorithmic pipeline is described as in Figure 4.

Conceptually, DPC tests the effect of one variable on the predictions of another, whilst taking into account all the rest of the variables at the same time. Hence it is able to monitor the dynamic process within reasonable computation time. It avoids linear model fitting and thus is more efficient and less constrained by the sample size. Note that a major difference between DPC and other

methods is, while others inspect the regression coefficients of full linear models, DPC takes advantage of the concept of Granger causality, based on a computationally fast method.

## Results

### Experiments on synthetic datasets

Since the ground truth is unknown for real expression data, comparisons of performance are first conducted on synthetic data and then on biological data.

Previously, SVAR and DBNs were experimentally proved to be useful using simulated data from autoregressive models [1,3]. These methods are based on the autoregressive model and their performance on other types of data is still not clear. When the data satisfies the model assumption, we can expect the corresponding technique to perform well. Therefore, an important question pertains to which assumption best describes gene expression data. In this section, we aimed to investigate the following question: how well the inference methods meet the requirements of microarray data?

The synthetic data generator GeneNetWeaver uses topologies generated based on real biological networks, therefore allowing good approximation of the statistical properties of real biological networks. It can sample from these transcriptional regulatory networks, and produce corresponding microarray datasets parameterized by the network topology, size of the network/number of genes, and type of experimental noise etc.

**Network topology.** Network topologies are generated by selecting sub-networks from a previously described *E. coli* network. Neighbouring genes are selected randomly among top 20% genes based on connectivity. This is to introduce stochasticity into gene selection. In this way, the resulting sub-network preserves features of scale-free networks such as modularity but it also allows the possibility of including small hubs and their targets. Consider, that one may want to model how the hub genes interact with their targets, but not all of the targets can be selected during the variable selection process. Therefore, sub-network generation by randomly selecting genes among the top 20% may represent a realistic situation in gene network analysis.

**Kinetic model.** After the topologies of the synthetic networks are sub-sampled from the *E. coli* transcriptional network, kinetic equations are selected for each gene and its regulators without

---

#### Algorithm 1 First-order directed partial correlation (DPC(1))

---

Construct the joint matrix  $\Phi = [\mathbf{Y}^+ \mathbf{Y}^-]$ , with  $\mathbf{Y}^+$  the present state ( $\mathbf{Y}^+ = \{\mathbf{Y}(u) | u \in 2 \dots \tau\}$ ) and  $\mathbf{Y}^-$  the past state ( $\mathbf{Y}^- = \{\mathbf{Y}(u) | u \in 1 \dots \tau - 1\}$ );

Compute the partial correlation matrix  $\mathbf{Q}_Y^{(1)}$  for the joint matrix  $\Phi$ ;

**for** each variable  $\mathbf{y}_k$  in  $\mathbf{Y}$  **do**

    Compute the partial correlation matrix  $\mathbf{Q}_{Y_{/k}}^{(1)}$  for the joint matrix with  $\mathbf{y}_k$  removed  $\Phi_{/k}$ ;

**for** each variable  $\mathbf{y}_i, i \neq k$  **do**

        Compute the influence of  $\mathbf{y}_k$  on  $\mathbf{y}_i$ ,  $e_{ki}$ , according to Eq. (9);

**end for**

**end for**

**for** each diagonal element  $e_{ii}$  in the directed partial correlation network probability matrix **do**

    Compute the partial correlation matrix  $\mathbf{Q}_{Y_{/i}}^{(1)}$  for the joint matrix with the lagged data  $\mathbf{y}_i^-$  removed  $\Phi_{/i-}$ ;

    Compute the effect of  $\mathbf{y}_i^-$  on  $\mathbf{y}_i$  according to Eq. (9).

**end for**

---

**Figure 4. The algorithmic pipeline for first-order DPC.** By avoiding linear model fitting it is thus more efficient and less constrained by the sample size.

doi:10.1371/journal.pone.0016835.g004

removing the autoregulatory relations. Different types of perturbations are applied to the networks, including multifactorial, dual knockout, knockout, and knockdown. We choose to model the gene network with ordinary differential equations. With this system the perturbations are applied at  $t=0$  and the statistical properties of the network do not depend on time.

**Experimental design.** In each run, we apply a method in comparison to a single gene expression time series dataset, e.g., a dataset with multifactorial perturbation, 500 genes, and 21 time points. In the DREAM challenge a team uses datasets of all four types of perturbations and multiple simulations to collectively infer a network. The DPC algorithm however, was formulated to deal with large numbers of genes and few time points. We found this situation underrepresented in the DREAM challenge datasets. For this reason we chose to use the DREAM challenge data simulator (GeneNetWeaver) to provide a more appropriate dataset for the assessment of this method. The simulations in this paper represent even more difficult problems for the inference methods. Specifically, for knockout and knockdown experiments, a simulation may see the change of expression profiles of very few genes while others remain constant. For this to be a standalone test, we then select the datasets based on the variance in the dataset and only use datasets with high variations.

**Parametrizing the simulations.** We simulate networks of size 50, 100, 200, and 500 genes with four types of perturbations. The time series are all simulated from time point 1 to 100, but measured with 21 time points or 100 time points to form two datasets with different time series lengths. Experimental noise is modeled by simulating noise in microarrays, which is a mix of normal and log normal noise. Then the data is normalized after the experimental noise is added. With 4 network sizes, 4 types of perturbations, 2 time series lengths, and 5 simulations for each setup, there are altogether  $4 \times 4 \times 2 \times 5 = 160$  datasets.

**Assessment metric.** Four multivariate time series inference algorithms as described above are evaluated in this experiment. Their ways of inferring the final network vary and each requires fine tuning for the parameters, which could be subjective for large-scale experiments (altogether 142 synthetic datasets are used). To eliminate any subjective elements and enable a fair comparison, we decided to compare directly on their preliminary output, the network probability matrices. For clarity, the related symbols for each probability matrix in the algorithms' technical details are listed in Table 1.

For the inferred network probability matrices, we compute their true positives (TP), false positives (FP), true negatives (TN), and false negatives (FN) at a given threshold. This procedure was

**Table 1.** Average consumed time of the four multivariate time series inference algorithms on the 100 time point datasets.

Method	DPC(1)	SVAR	GC-VAR	DBNs
Score matrix	$e^{(t)}$	$ r $	$\mathbf{g}$	$P_{max}$
Average time (second)				
50 × 100	3.275	0.545	144.247	256.684
100 × 100	12.887	1.856	N/A	2065.752
200 × 100	59.164	8.112	N/A	N/A
500 × 100	626.075	81.646	N/A	N/A

doi:10.1371/journal.pone.0016835.t001

repeated 500 times for each test statistic and variance scenario to obtain Receiver Operator Characteristic (ROC) curves [15,16] for describing the dependence of true positive rate  $TPR = TP / (TP + FN)$  and false positive rate  $FPR = TN / (TN + FP)$ . ROC curves provide a straightforward graphical representation of the performance of the algorithms. They are especially useful in comparisons by using many thresholds. As a summary metric for ROC, the area under the ROC curve (AUC), as its name indicates, measures the average accuracy of the prediction.

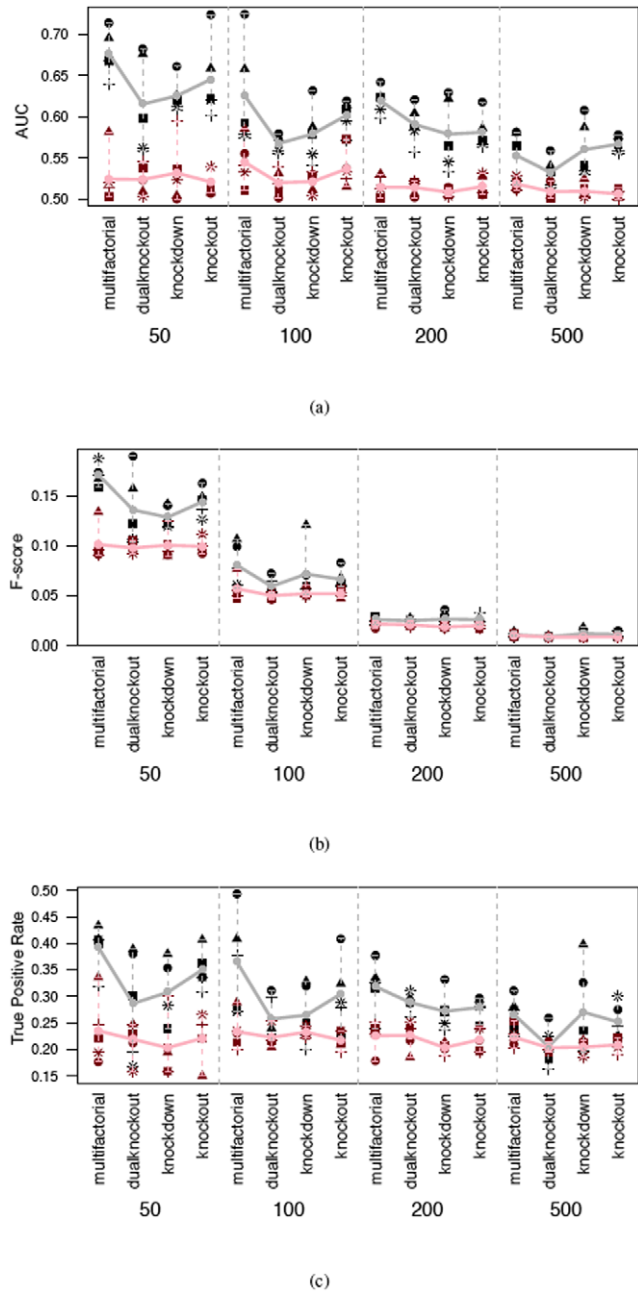


**Figure 5.** Performance scores of two network inference algorithms (black/grey: DPC, red/pink: SVAR) when tested on datasets with 50, 100, 200, and 500 genes respectively and 21 time points. The symbol denotes the identity of the five simulations, and the lines denote the average of simulation results. (a) AUC values, (b) F-score, (c) TPR at FPR of 0.2.

doi:10.1371/journal.pone.0016835.g005

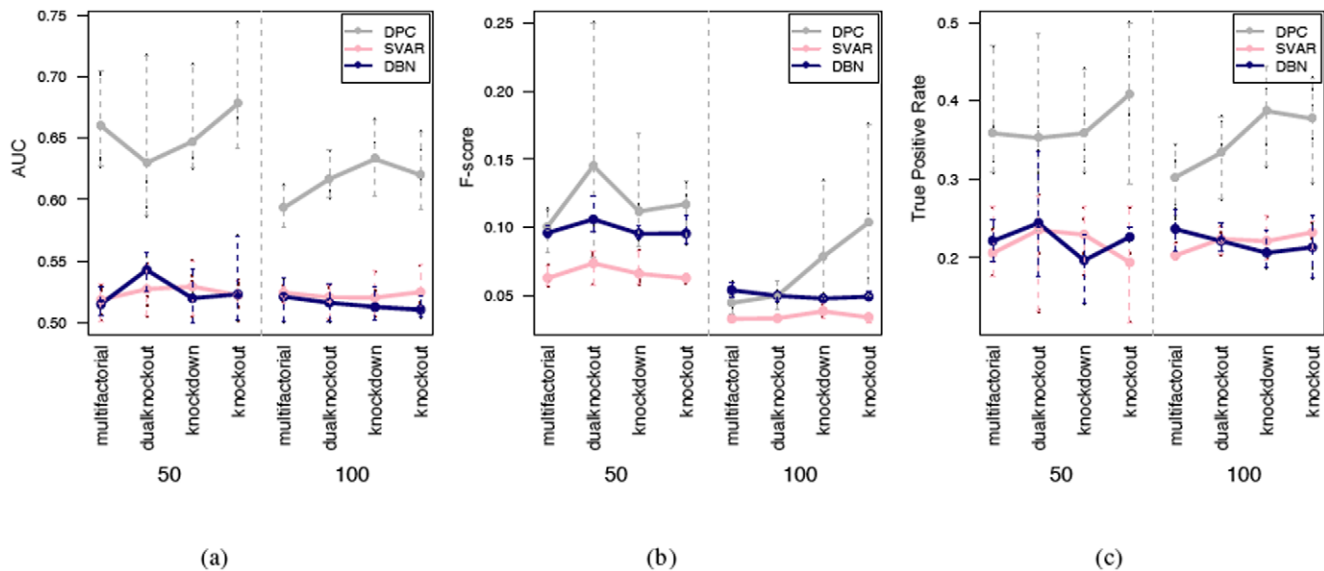


**Figure 6. Performance scores of three network inference algorithms when tested on 50 and 100 gene networks with 21 time points.** (a) AUC values, (b) F-score, (c) TPR at FPR of 0.2. doi:10.1371/journal.pone.0016835.g006

While AUC provides a quantitative measurement on the average performance for a method, maximum F-score [17] evaluates each method at its point of optimum performance. F-score is the harmonic mean of precision ( $TP/(TP+FP)$ ) and recall ( $TP/(TP+FN)$ ). In the implementation we use a balanced harmonic mean of precision and recall. As a composite measure, the F-score penalises algorithms with higher specificity and rewards algorithms with higher sensitivity.

Apart from these metrics, we also base our evaluation on the consumed computation time and the true positive rate at a 0.2 false positive rate, since usually a low false positive rate is preferred. All three metrics are used for assessment in the simulation experiments.

**Experimental results.** For DPC and SVAR, we plot their experimental results together so that they can be compared with respect to individual simulations. Then the average results on part of the datasets for each of the four algorithms are shown in separate plots. This is because GC-VAR can only be applied on datasets with 100 time points and 50 genes, since it requires long time series ( $t \gg n$ ) to fit linear models. Because of the high computational costs of DBNs, we only compute its results for networks of size 50 and 100 for both the 21 time point and 100 time points datasets.

With 21 time points, quantitative measurements of performance including AUC values, and F scores and true positive rates at 0.2 false positive rate for SVAR and DPC are provided in Figure 5. It is easy to observe a descent in their performances as network size increases. This is expected for difficult inference tasks with low signal-to-noise ratio. In these simulations, the true signal as a result of the initialization of perturbation, often on a single gene, is easily buried among the experimental noise. Nevertheless, in comparison DPC shows superior performance in the results. Following, the results as the average of the outcome of simulations of same setting Figure 6 compares the performance of DPC, SVAR and DBN, with error bars showing the range of results. Here again, DPC achieves the best results.

With 100 time points, DPC also outperforms SVAR in terms of AUC, F-scores, and the true positive rates at 0.2 false positive rate

(Figure 7). Comparing results from the 21 time point experiments (Figure 5) and the results from the 100 time points experiments (Figure 7), the influence of sample sizes on the performance can be observed. This conforms to current theory and is reassuring. Then measurements of the performance of all four methods on part of the 100 time point datasets is shown in Figure 8. From the average result, GC-VAR and DBN only outperform SVAR for the 50 gene network, while DPC is the best performer. The average consumed time for the 100 time point datasets is given in Table 1 on a Mac Pro ( $2 \times 2.26$  GHz). For the 21 time points datasets consumed time is similar with the results in this table and hence is not shown. From this table, a noticeable advantage of DPC can be seen in its efficiency, although SVAR is the most efficient.

**A note on the performance.** Several state-of-the-art methods have also been tested but showed poor performance on the GNW benchmarks (data not shown). This may be because some perturbations have only few downstream effects. When the regulators are not perturbed, the real relationships between them and their downstream targets cannot be found. Effectively, a significant proportion of the variation in the data is a result of experimental noise. Hence for some inference methods, it is difficult to pick up the true signals amidst noise.

In DREAM an *in silico* challenge provides four perturbations each of 10 simulations to infer a network. However, for benchmarking in this paper we use a single simulation for one type of perturbation as input. As a result, better performance in DREAM can be expected for the methods in comparison. Nevertheless, for comparative purposes, these simulation assessments undoubtedly yield benchmarking results on a fair ground, i.e. not biased towards any model assumptions.

### Experiments on a biological dataset

To test these methods' performance on biological data, a *Arabidopsis L. Heynith* dataset [18] of 800 genes and 22 time points is used. The data is collected from an experiment investigating the impact of the diurnal cycle of the starch metabolism in the leaves of *Arabidopsis*. Two replicates consist of measurements at 11 time

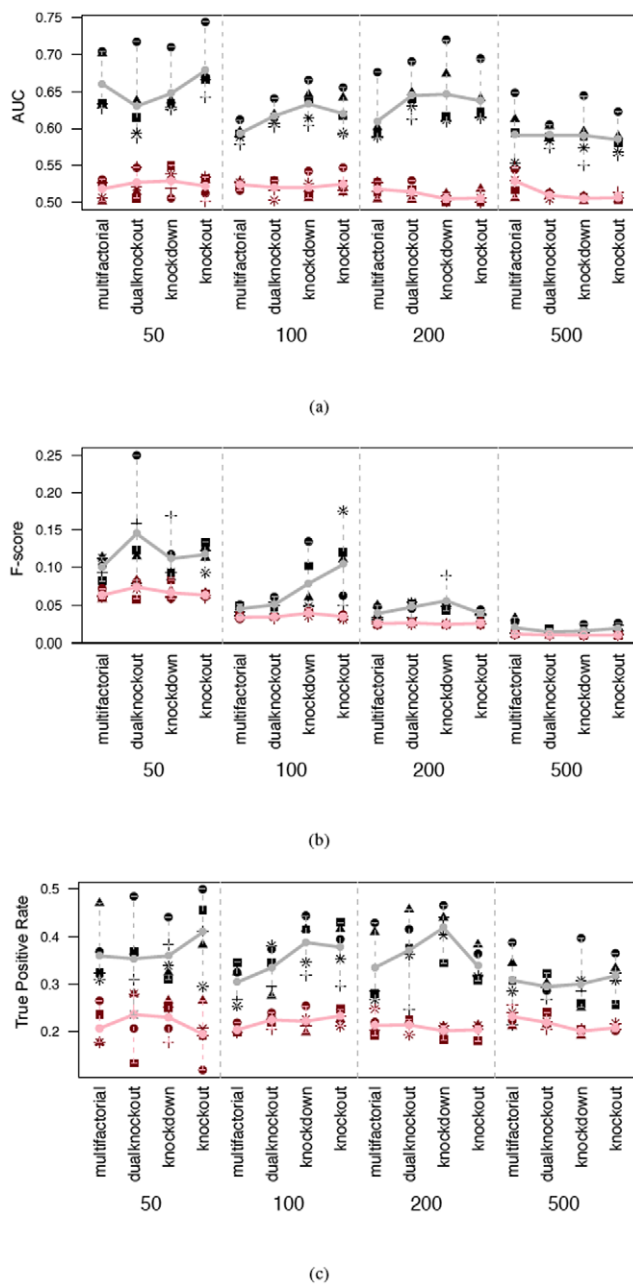


**Figure 7. Performance scores of two network inference algorithms (black/grey: DPC, red/pink: SVAR) when tested on networks with 50, 100, 200, and 500 genes respectively and 100 time points.** (a) AUC values, (b) F-score, (c) TPR at FPR of 0.2. doi:10.1371/journal.pone.0016835.g007

points of uneven time intervals to capture the periods immediately after the transitions from dark (light) to light (dark). Samples were firstly taken at the end of light period, then at 1, 2, 4, 8, and 12 hr of darkness and at 1, 2, 4, 8, and 12 hr of light. During the day, starch is synthesised to serve as an intermediate store of carbon fixed during photosynthesis when rates of production exceed the export rates of the chloroplasts. During the night, starch formed and stored within the chloroplasts during the day is metabolized to maltose and glucose and exported from the chloroplast. These exported breakdown products are then used as sources of energy for plant growth and metabolism as well as being sent to sink tissues where starch can be re-synthesised for more long term

storage in specialised storage organelles called Amyloplasts (for a detailed review see [19]).

For the assessment of our validation scheme, a subset of 800 genes is used which was previously selected using a periodicity test [20] and was first studied by Rhein and Strimmer for gene network inference [1].

Given the sample size and network size, GC-VAR and DBN cannot be applied to this dataset. DPC and SVAR are applied to produce resulting probability matrices. We compare the probability matrices by using two validation methods as below. As the length of time series is short, we choose  $p=0$  for DPC.

**Validation with SAMBA for extracting network modules.** A biclustering method is adopted as part of the validation process. Biclustering aims to find a group of variables that share similar data patterns under a subset of conditions. When applied to expression data, it searches for a group of genes with similar expression patterns under a subset of conditions/treatments. But when applied to probability matrices that indicate regulatory interactions, as described previously in [21], it searches for a subset of genes with similar regulatory patterns whilst under the regulatory influence of a second subset of genes, as illustrated in Figure 9. In other words, biclustering can be applied to probability matrices to get statistically significant submatrices, which are equivalent to network modules in our case.

With probabilistic modeling and graph theory techniques, SAMBA [22] identifies subsets of rows of a matrix that jointly respond in a similar manner across subsets of columns. The biclusters are allowed to be overlapped. In our experimental design, each value in the probability matrices indicates whether a gene corresponding to a row regulates a gene in a column. The resulting biclusters of the probability matrix correspond to regulatory network modules, with rows corresponding to groups of regulatory genes regulating sets of target genes in the columns. Therefore SAMBA provides an efficient way of validating network inference algorithms. One main advantage of this method is that, by allowing overlapping modules/biclusters, regulators and targets are allowed to appear in different network modules. This satisfies the biological assumption that genes may have multiple functions and can be involved in different pathways. Also, it allows multiple regulators to exert their potential regulatory influences in hierarchical or co-dependant manners on particular subset of targets.

247 biclusters were found for the DPC matrix with quality scores of 88–2277 (mean = 260.8, sd = 219.7), while 257 biclusters were found for SVAR with quality scores of 87–940 (mean = 233.5, sd = 102.8). GO [23] and promoter enrichment were computed for each of the biclusters, as listed in Table S1 and S2 for DPC and SVAR. In summary, the DPC biclusters are enriched with 47 GO terms, while the SVAR biclusters are enriched with 24 GO terms (corrected  $p \leq 0.05$ ). The fact that DPC presents more GO terms for its biclusters than SVAR suggests that DPC is inferring more fundamentally accurate regulatory interactions, which in turn results in biclusters/regulatory modules of targets which are more likely to be co-regulated members of the same biological process or pathway. Several GOs (chloroplast - GO:0009507; plastid - GO:0009536; organelle envelope - GO:0031967; organelle membrane - GO:0031090; organelle subcompartment - GO:0031984; and photosynthesis - GO:0015979) identified by both DPC and SVAR suggest that the biclusters represent modules of genes with potential roles in diurnal starch metabolism. In addition, one GO term identified in two biclusters from the DPC results and not SVAR is starch metabolic process - GO:0005982. This is a highly informative GO considering the biological process under investi-



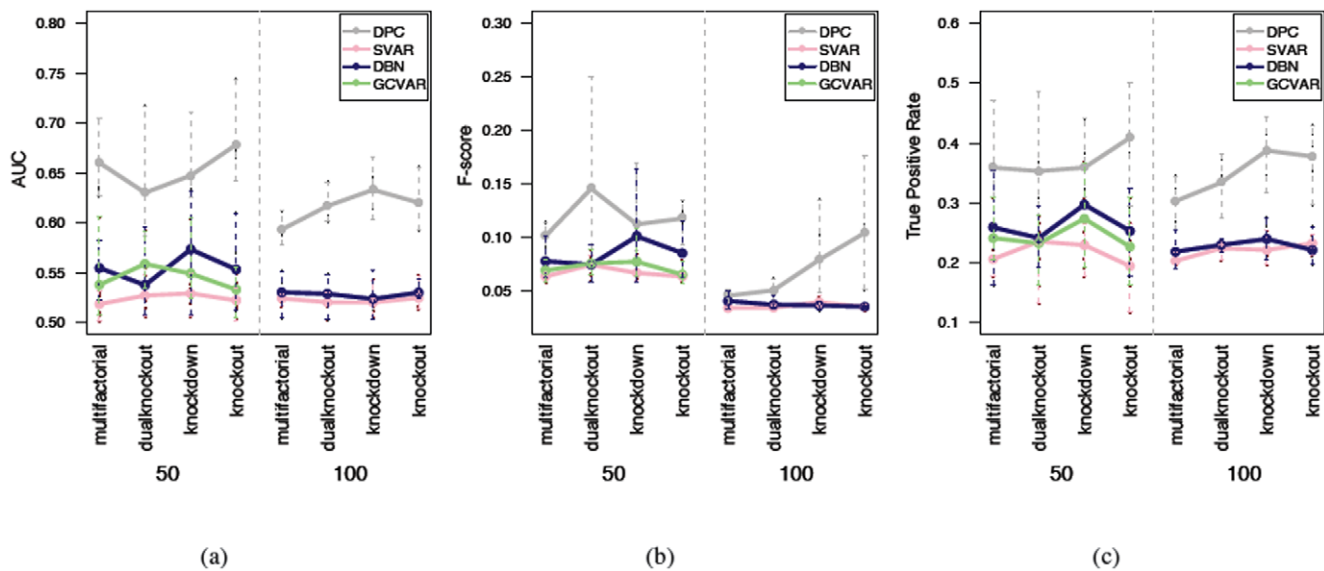


**Figure 8. Performance scores of four network inference algorithms when tested on datasets of tested on 50 and 100 gene networks with 100 time points.** (a) AUC values, (b) F-score, (c) TPR at FPR of 0.2. doi:10.1371/journal.pone.0016835.g008

gation [18], suggesting that perhaps DPC is uncovering more biologically relevant gene-gene associations from the data.

Enrichment analysis is performed for transcription factor binding elements in target promoters. 60 cases of promoter enrichment were observed for DPC biclusters while 44 cases were identified in the SVAR biclusters ( $p \leq 0.001$ ). Lists of promoter enrichments are provided in Table S3 and S4 for DPC and SVAR. Again, in spite of the observation that SVAR produced more biclusters than DPC, the results suggest that DPC gives rise to more intuitive groupings of genes, as we would expect co-regulated genes to share common binding motifs in their promoters, where transcription factors that are involved in their co-ordinated regulation can bind.

**An interesting starch deregulation bicluster.** More interestingly, one bicluster of the DPC network was found to have several members of the starch degradation pathway active in the chloroplasts in the dark. This bicluster (number 190 as shown in Figure 10), has about 27 members where 5 of these (Figure 10(a)) are known to be involved in starch degradation and two more with

potential involvement in this process due to familial relationships with known components of this pathway [19]. Of the 48 genes investigated in [18], 10 of these were included in this 800-gene dataset.

In particular, AMY3 (At1g69830), ISA3 (At4g09020), PHS1 (At4g29320) and SEX1/GWD1 (At1g10760) are known to be part of the starch degradation pathway operating in chloroplasts [19]. In addition, two other members PHS2 (At3g46970) and DPE2 (AT2g40840) with their paralogous relationships to the pathway described above also present interesting information regarding their potential co-ordinated regulation with the four chloroplast components (Figure 10(c)). Furthermore, this cluster also contains COR15B (At2g42530) while its homologue COR15A (At2g42540) is a suggested regulator of the bi-cluster. Both proteins are induced by cold stress and abscisic acid treatment [24], while COR15A has been shown to be present in chloroplasts [25]. Another proposed regulator of this bi-cluster is the uncharacterised MYB transcription factor (At1g58220) which is interesting considering several MYBs have been implicated in regulating photosynthesis under stress [26].

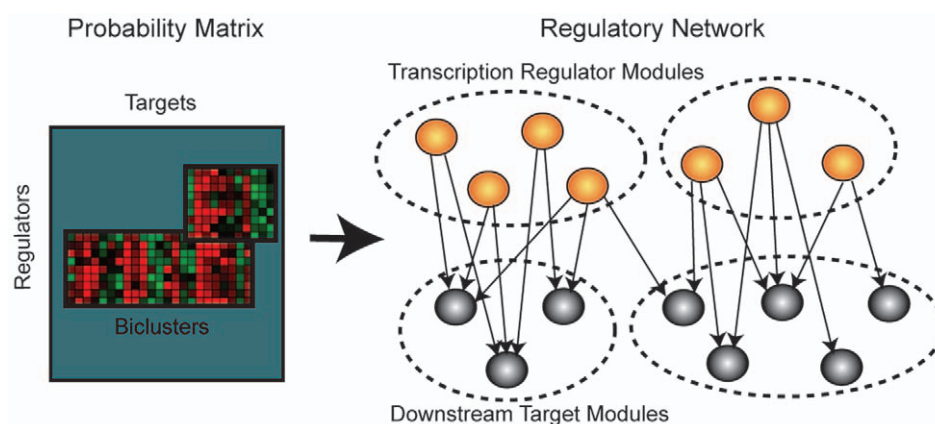


**Figure 9. Biclustering a network probability matrix is equivalent to pulling out network modules.** Because coefficients in the biclusters are highly correlated, it means genes in rows and columns share similar regulatory patterns. doi:10.1371/journal.pone.0016835.g009

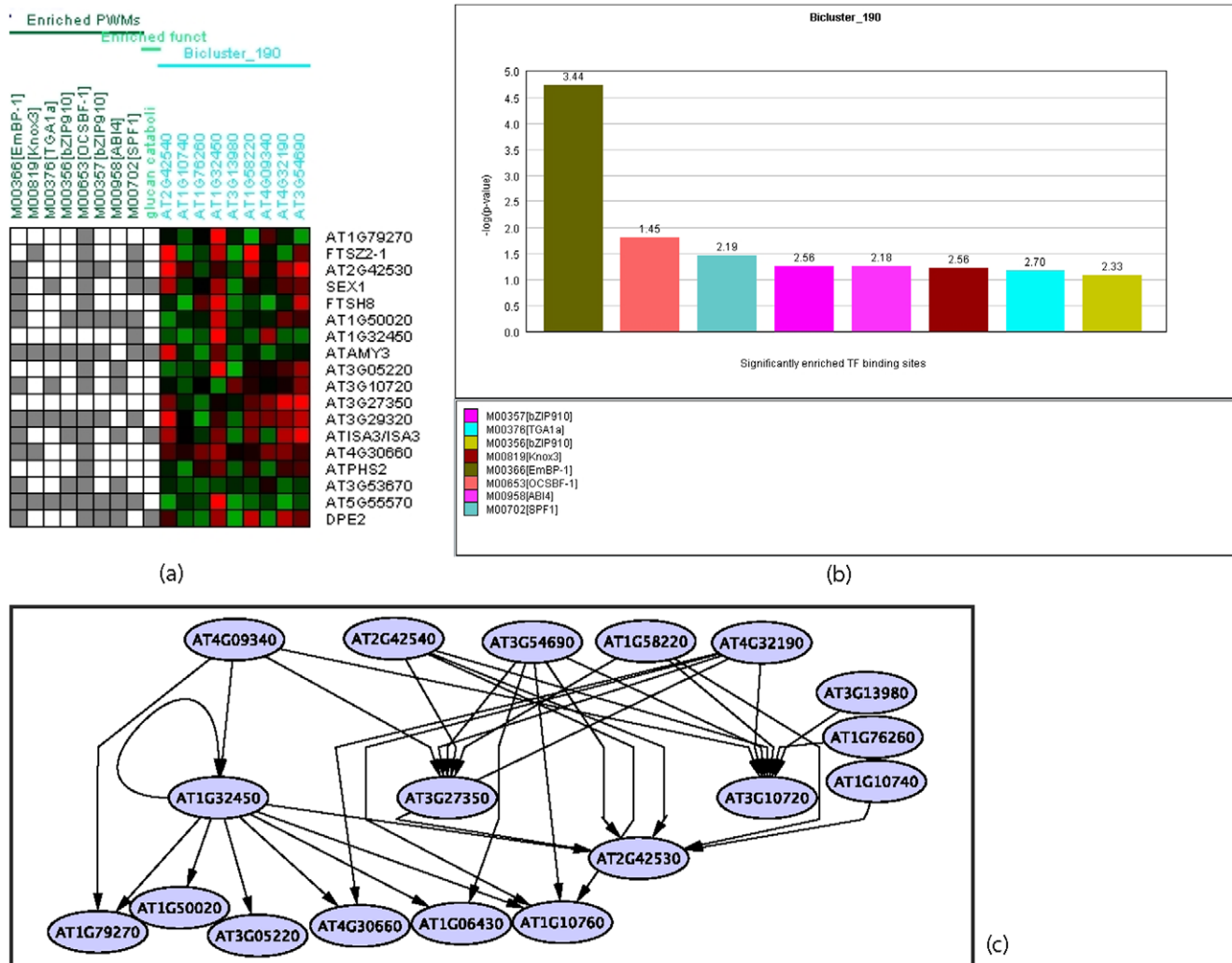


**Figure 10. New information can be derived from a bicluster 190 combining biological knowledge and DPC network.** (a) Heatmap of the bicluster number 190 of the DPC network probability matrix. (b) Significantly enriched motifs in this bicluster. (c) A visual representation of the interactions predicted by DPC(1) between the members of bicluster 190. While statistically not the strongest interactions resolved within the 800 gene set, the biological association of the co-regulated targets none the less indicates that the biclustering has helped to reveal weaker but far more pertinent signals of potential co-ordinated regulation. These relationships would otherwise have been lost if a rudimentary ranking of the strengths of the interactions had been used instead. doi:10.1371/journal.pone.0016835.g010

The tight grouping of these genes within the large background subset of genes indicates that DPC appears to be identifying target genes which are potentially co-regulated and involved in the same biological pathway. A larger bicluster (number 222), containing 43 members identified within the SVAR data was also found to contain 3 of the 5 known genes and the two putative pathway members identified in the DPC bicluster number 190. From the validation results it appears that DPC generates more biologically meaningful results than SVAR.

One of the significantly enriched motifs in bicluster 190 one motif M00958 (Figure 10(b)) suggests that ABI4, a transcription factor known to influence photosynthesis and starch regulation in response to ABA and sugar signalling [27] may play an important regulatory role. There is also a further interesting level of correlation given that the proposed target COR15B and the proposed regulator COR15A in this bicluster are both transcriptionally induced following exogenous application of ABA [24].

**Validation with transcription regulators as network hubs.** Besides analysing the biclustering results, we also looked

directly for known regulators. 41 of the 800 genes are known transcription factors in Arabidopsis. Since a row of coefficients in the probability matrix represents probabilities of one gene regulating other genes, the sum of this row should be proportional to the probability of this gene being a regulator. A Welch-Satterthwaite test [28] is performed to compare two groups with the alternative hypothesis that the mean of one group is greater than the other: the rows of the probability matrix for the 41 transcription factors is compared against all of the probability matrix. The more significantly different the two groups are, the better the probability matrix differentiates between known transcription factors and other genes. Therefore, the method that better captures the underlying network structure is the one with the more significant result from this t-test. The resulting p-values are  $1.0 \times 10^{-14}$  for SVAR and  $2.2 \times 10^{-16}$  for DPC, indicating that DPC is better in capturing the network structure with respect to these hubs.

The 41 transcription factors are then tested individually for their roles in the probability matrices of DPC and SVAR in the same

way. Results of the test are provided in Table S5 and S6 for DPC and SVAR, respectively. The well known circadian regulators LHY and CCA1 [29,30] are regarded as transcription factors by DPC (both have corresponding  $p=0$ ). Test results for SVAR are 0.358 and 0.927, respectively. Further, promoter analysis in the region of  $-1,000$  to  $200$  bp of the downstream targets is performed for both of the potential hubs. To conduct the comparison on a fair ground, we take the 30 most significantly interacting genes with LHY and CCA1 in both cases for SVAR and DPC. For SVAR, promoters of putative CCA1 targets are enriched with 7 motifs with p-values ranging from  $1.2E-14$  to  $9.3E-12$ . Promoters of putative LHY targets are enriched with 10 motifs with p-values from  $1.3E-14$  to  $7.6E-12$ . For DPC, promoters of putative CCA1 targets are enriched with 6 motifs with p-values ranging from  $1.4E-14$  to  $7.5E-12$ , and promoters of putative LHY targets are enriched with 10 motifs with p-values from  $1.0E-15$  to  $4.7E-12$ . In particular, the motif with p-value  $1.0E-15$  in promoters of putative LHY targets (Figure S1), as determined by DPC, is close to a known motif HSF(M00028). As both of these methods identified similar numbers of motifs no real conclusion can be drawn as to which method is superior in this respect, as both methods may have uncovered equally valid binding motifs. Here we are also limited by the number of biologically determined motifs for which there exist probability weight matrices. Such that the presence of the known motif HSF(M00028) should not mitigate the importance of the other motifs which are equally plausible until otherwise experimentally disproved. Nonetheless the above analyses of the biological dataset have presented many interesting possibilities concerning the transcriptional regulation of diurnal starch metabolism which warrant further experimental investigation. Overall, DPC appears to reveal more biologically intuitive and plausible regulatory scenarios.

## Discussion

This paper reviews some recent advances in multivariate time series inference of gene expression data. It then reports a new method, Directed Partial Correlation (DPC), for efficient and effective large-scale network inference. Experiments on both simulated and biological data are designed to investigate the properties of the proposed method and existing methods.

From the experimental results, superior performance of the proposed DPC method is observed when compared to three other inference methods. When analyzing simulated datasets, DPC can pick up the true signal and reveal the underlying relationships. SVAR is the most efficient, but less effective than DPC in most of the cases. For the biological dataset, DPC appears to give more biological meaningful results than SVAR. These results provide good evidence that DPC is suitable for the scenario of expression time series analysis.

## References

- Opgen-Rhein R, Strimmer K (2007) Learning causal networks from systems biology time course data: an effective model selection procedure for the vector autoregressive process. *BMC Bioinformatics* 8: S3.
- Bernard A, Hartemink AJ (2005) Informative structure priors: joint learning of dynamic regulatory networks from multiple types of data. *Proceedings of the Pacific Symposium on Biocomputing*. pp 459–70.
- Lebre S (2009) Inferring dynamic genetic networks with low order independencies. *Statistical Applications in Genetics and Molecular Biology* 8.
- Granger CWJ (1969) Investigating causal relations by econometric models and cross-spectral methods. *Econometrica* 37: 424–438.
- Zou C, Feng J (2009) Granger causality vs. dynamic bayesian network inference: a comparative study. *BMC Bioinformatics* 10: 122+.
- Marinazzo D, Pellicoro M, Stramaglia S (2008) Kernel-granger causality and the analysis of dynamical networks. *Physical Review E (Statistical, Nonlinear, and Soft Matter Physics)* 77.
- Schäfer J, Strimmer K (2005) An empirical Bayes approach to inferring large-scale gene association networks. *Bioinformatics* 21: 754–64.
- Veiga D, Vicente F, Grivet M, de la Fuente A, Vasconcelos A (2007) Genome-wide partial correlation analysis of escherichia coli microarray data. *Genet Mol Res* 6: 730–742.
- Marbach D, Schaffter T, Mattiussi C, Floreano D (2009) Generating Realistic In Silico Gene Networks for Performance Assessment of Reverse Engineering Methods. *Journal of Computational Biology* 16: 229–239.
- Stolovitzky G, Monroe DON, Califano A (2007) Dialogue on reverse-engineering assessment and methods: The dream of high-throughput pathway inference. *Annals of the New York Academy of Sciences* 1115: 1–22.
- Ltkepohl H (2006) *New Introduction to Multiple Time Series Analysis*. Springer Publishing Company, Incorporated.
- Mukhopadhyay NDD, Chatterjee S (2006) Causality and pathway search in microarray time series experiment. *Bioinformatics*.

Additionally, we should be aware that high-throughput data often lacks the specificity for accurate inference of regulatory relationships. Therefore, the network inference result can be either examined in a modular fashion as in the paper, or combined with other data sources or biological knowledge to address complex biological problems.

In summary, the proposed DPC algorithm has excellent performance with large numbers of variables. Its efficiency in learning among hundreds of variables is mainly due to the fact that the computation is based on partial correlation instead of model fitting. DPC has the potential of being extended to applications on static data such as cancer expression for learning the data structure. With time series data, the time lag should be carefully selected based on users understanding of the dataset, in order to reveal the information embedded in time lags.

## Supporting Information

**Figure S1** A significantly enriched motif in LHY targets as determined by DPC in network module/bicluster 190. (TIF)

**Table S1** GO enrichment for DPC biclusters (Bonferroni adjusted  $p$ -value  $\leq 0.05$ ). (XLS)

**Table S2** GO enrichment for SVAR biclusters (Bonferroni adjusted  $p$ -value  $\leq 0.05$ ). (XLS)

**Table S3** Transcription factor enrichment for DPC biclusters ( $p$ -value  $\leq 0.001$ ). (XLS)

**Table S4** Transcription factor enrichment for SVAR biclusters ( $p$ -value  $\leq 0.001$ ). (XLS)

**Table S5** Transcription regulators ranking by SVAR. (TXT)

**Table S6** Transcription regulator ranking by DPC(1). (TXT)

## Acknowledgments

The authors are grateful to the anonymous reviewers for their insightful comments and valuable suggestions. We thank Thomas Schaffter and Daniel Marbach for their advices on data simulations.

## Author Contributions

Conceived and designed the experiments: YY. Performed the experiments: YY. Analyzed the data: YY OW. Wrote the paper: YY CL OW.

13. Benjamini Y, Hochberg Y (1995) Controlling the false discovery rate: A practical and powerful approach to multiple testing. *Journal of the Royal Statistical Society B*: 289–300.
14. Bro R, Sidiropoulos ND, Smilde AK (2002) Maximum likelihood fitting using ordinary least squares algorithms. *Journal of Chemometrics* 16: 387–400.
15. Egan J (1975) Signal detection theory and ROC analysis, Series in Cognition and Perception. New York, NY, USA: Academic Press.
16. Fawcett T (2006) An introduction to roc analysis. *Pattern Recogn Lett* 27: 861–874.
17. Rijsbergen CJV (1979) Information Retrieval. Newton, MA, USA: Butterworth-Heinemann.
18. Smith S, Fulton D, Chia T, Thorncroft D, Chapple A, et al. (2004) Diurnal changes in the transcriptome encoding enzymes of starch metabolism provide evidence for both transcriptional and posttranscriptional regulation of starch metabolism in arabidopsis leaves. *Plant Physiology* 136: 2687–2699.
19. Zeeman SC, Smith SM, Smith AM (2007) The diurnal metabolism of leaf starch. *Biochem J* 401: 13–28.
20. Wichert S, Fokianos K, Strimmer K (2004) Identifying periodically expressed transcripts in microarray time series data. *Bioinformatics* 20: 5–20.
21. Lee H, Kong SW, Park PJ (2008) Integrative analysis reveals the direct and indirect interactions between dna copy number aberrations and gene expression changes. *Bioinformatics* 24: 889–896.
22. Tanay ASR, Sharan R (2002) Discovering statistically significant biclusters in gene expression data. *Bioinformatics* 18(1): S136–144.
23. The Gene Ontology Consortium (2000) Gene ontology: tool for the unification of biology. *Nature Genetics* 25: 25–29.
24. Wilhelm KS, Thomashow MF (1993) Arabidopsis thaliana cor15b, an apparent homologue of cor15a, is strongly responsive to cold and aba, but not drought. *Plant Mol Biol* 23: 1073–7.
25. Lin C, Thomashow MF (1992) Dna sequence analysis of a complementary dna for cold-regulated arabidopsis gene cor15 and characterization of the cor 15 polypeptide. *Plant Physiol* 99: 519–525.
26. Saibo NJM, Lourenco T, Oliveira MM (2009) Transcription factors and regulation of photosynthetic and related metabolism under environmental stresses. *Ann Bot* 103: 609–623.
27. Rook F, Hadingham SA, Li Y, Bevan MW (2006) Sugar and aba response pathways and the control of gene expression. *Plant Cell Environ* 29: 426–34.
28. Welch BL (1947) The generalization of “student’s” problem when several different population variances are involved. *Biometrika* 34: 28–35.
29. Schaffer R (1998) The late elongated hypocotyl mutation of arabidopsis disrupts circadian rhythms and the photoperiodic control of flowering. *Cell* 93: 1219–1229.
30. Wang ZY, Kenigsbuch D, Sun L, Harel E, Ong M, et al. (1997) A myb-related transcription factor is involved in the phytochrome regulation of an arabidopsis lhcb gene. *PlantCell* 9: 491–507.